

Ethylation of benzene: Effect of zeolite acidity and structure

T. Odedairo, S. Al-Khattaf*

Center of Excellence in Petroleum Refining and Petrochemicals, King Fahd University of Petroleum & Minerals, Dhahran 31261, Saudi Arabia

ARTICLE INFO

Article history:

Received 22 April 2010

Received in revised form 1 June 2010

Accepted 18 June 2010

Available online 25 June 2010

Keywords:

Zeolites

Benzene ethylation

Ethylbenzene

Kinetic modeling

ABSTRACT

Zeolite catalysts based on ZSM-5, TNU-9, SSZ-33 and mordenite were prepared and characterized. The catalytic performance of these zeolites containing channels of different sizes has been studied in benzene ethylation with ethanol at three different reaction temperatures (250, 275 and 300 °C) for reaction times of 3, 5, 7, 10, 13, 15 and 20 s. In the ethylation reaction of benzene with ethanol, SSZ-33 catalyst comprising 12-12-10-ring channels gave the highest benzene conversion, which is the result of high acidity of this zeolite together with increased mass transport through large pores. The conversion of benzene in the ethylation reaction of benzene with ethanol over the different zeolite catalysts follows the order: SSZ-33 > TNU-9 > ZSM-5 > mordenite. TNU-9 catalyst behaves like the 10-ring ZSM-5 with respect to ethylbenzene selectivity, while the behavior of SSZ-33 is close to that of a large pore zeolite with potential cage effects. EB selectivity follows the order: ZSM-5 > TNU-9 > SSZ-33 > mordenite, which implies that this order is not directly related to the benzene conversion. In addition, a simplified kinetic model based on reactant-converted deactivation model was developed for the reaction and compared with the obtained experimental data.

© 2010 Elsevier B.V. All rights reserved.

1. Introduction

Ethylbenzene (EB) is important in the petrochemical industry as an intermediate in the production of styrene, which in turn is used for making polystyrene, a commonly used plastic material [1]. The 90% of EB world's production is employed in the manufacture of styrene, the other 10% is used in other applications like paint solvents and pharmaceuticals [2]. The world's more than 90% of ethylbenzene demand is met through benzene ethylation. Ethylbenzene is produced in bulk quantities by alkylation of benzene with ethene in the presence of aluminium chloride or zeolite catalyst [3]. Conventionally, ethylbenzene is produced by benzene alkylation with ethylene using homogeneous mineral acids such as aluminium chloride or phosphoric acid as catalysts that cause a number of problems concerning handling, safety, corrosion and waste disposal [4,5]. The use of zeolite catalysts offers an environmentally friendly route to ethylbenzene and the possibility of achieving superior product selectivity through pore size control [6,7]. Lately, Zilkova et al. [8] reported the role of the zeolite channel architecture and acidity on the activity and selectivity in aromatic transformation.

Recently, aluminium chloride catalyzed alkylation of benzene with ethene has been replaced by zeolite-catalyzed alkylation processes [9]. Starting from the mid 1960s different zeolite-based

catalysts were extensively evaluated for benzene alkylation using various alkylating agents [10–14]. The direct use of ethanol, instead of ethene, as alkylating agent with benzene for this reaction has gained more attention [15–17]. A long stable catalyst life is observed when alcohol, rather than ethylene, is used as an alkylating agent [18]. Zeolite ZSM-5 was reported to be active in the ethylation of benzene and toluene [19–22], which led to the great commercial process (Mobil–Badger). In addition, the effect of zeolite acidity in benzene and toluene alkylation has also been reported by various researchers [23,24]. More recently, mordenite is used in the adsorptive separation of gas or liquid mixtures and catalysis such as hydrocracking, hydroisomerization, alkylation, reforming, dewaxing and dimethylamines synthesis due to its high thermal and acid stabilities [25–27]. In addition, MOR zeolite has recently been considered for applications as hosts of semiconductor materials, chemical sensors and nonlinear optical materials [28].

A very important investigation of alkylation of benzene with ethanol by Levesque and Dao [29] over steamed-treated ZSM-5 zeolite and chryso-zeolite ZSM-5 catalysts showed that ethylbenzene selectivity increased at high benzene to ethanol molar ratio. Gao et al. [30] studied the alkylation of benzene with ethanol over ZSM-5-based catalyst. They investigated the effect of zinc salt on the synthesis of ZSM-5 in the alkylation of benzene with ethanol. They concluded that the increase in EB selectivity was due to high Lewis/Bronsted acid ratio and the smaller crystal size. Chandawar et al. [31] also studied the alkylation of benzene over modified ZSM-5-based catalyst. The authors reported a significant improvement in ethylbenzene selectivity.

* Corresponding author. Tel.: +966 3 860 1429; fax: +966 3 860 4234.
E-mail address: skhattaf@kfupm.edu.sa (S. Al-Khattaf).

Nomenclature

| | |
|------------------------------|---|
| C_i | concentration of specie i in the riser simulator (mol/m ³) |
| CL | confidence limit |
| E_i | apparent activation energy of i th reaction (kJ/mol) |
| k_1 | rate constant of reaction 1 (m ³ /kg of catalyst .s) |
| k_2 | rate constant of reaction 2 (m ³ /kg of catalyst .s) |
| k_3 | rate constant of reaction 3 (m ³ /kg of catalyst .s) |
| k_4 | rate constant of reaction 4 (m ³ /kg of catalyst .s) |
| k | apparent kinetic rate constant (m ³ /kg of catalyst .s) |
| k_0 | pre-exponential factor in Arrhenius equation defined at an average temperature [m ³ /kg of catalyst .s], units based on first-order reaction |
| MW _{i} | molecular weight of specie i |
| R | universal gas constant (kJ/kmol K) |
| t | reaction time (s) |
| T | reaction temperature (K) |
| T_0 | average temperature of the experiment (275 °C) |
| V | volume of the riser (45 cm ³) |
| W _c | mass of the catalysts (0.81 g cat) |
| W _{hc} | total mass of hydrocarbons injected in the riser (0.162 g) |
| Y_i | mass fraction of i th component (wt%) |

Greek letters

| | |
|-----------|---|
| φ | apparent deactivation function |
| λ | catalyst deactivation constant (RC Model) |
| η | effectiveness factor, dimensionless |

Subscripts

| | |
|-----|----------------------|
| 0 | at time $t=0$ |
| 1 | for reaction (1) |
| 2 | for reaction (2) |
| 3 | for reaction (3) |
| 4 | for reaction (4) |
| cat | catalyst |
| i | for i th component |

Abbreviations

| | |
|-----|----------------|
| B | benzene |
| DEB | diethylbenzene |
| E | ethanol |
| EB | ethylbenzene |
| T | toluene |
| P/O | para to ortho |

In a recent publication, Odedairo and Al-Khattaf [32] investigated the ethylation of benzene with ethanol over ZSM-5-based catalyst. It was found that, the reaction proceeded via two alkylation steps producing EB and diethylbenzene (DEB), respectively. The apparent activation energy for benzene ethylation was found to be 32.28 kJ/mol.

Several researchers have reported the studies on alkylation reactions over ZSM type zeolites, [33–36] but only a few researchers have performed alkylation reactions over mordenite-zeolite. Young [21] reported alkylation of benzene over H-ZSM-12 and H-mordenite dealuminated by HCl. The author obtained a benzene conversion of 98% over H-mordenite and a conversion of 54% over H-ZSM-12. Recently, Wang et al. [37] reported the alkylation of benzene over a commercial mordenite, which contained 30% Al₂O₃ as the binder, was studied in a fixed-bed reactor at over 1.0 MPa and a conversion of 95% was achieved.

Odedairo and Al-Khattaf [38] also studied the ethylation of benzene over Y-zeolite-based catalysts. Toluene was reported to be one of the major products, which was formed as a result of EB cracking.

Zeolite SSZ-33 (CON topology) possesses a channel system comprised of intersecting 12-ring and 10-ring pores; it is the first synthetic zeolite having 4-4 = 1 SBU (secondary building unit) in the structure [39]. Recently, Corma et al. [40] studied the alkylation of benzene with ethanol over SSZ-33 in comparison with other zeolite-based catalysts. They found that the activity of SSZ-33 for the conversion of ethanol and benzene is the highest among the four zeolites studied, while the activity of the others (ZSM-5, Beta/Ge and ITQ-22) is very similar.

TNU-9 represents a new three-dimensional zeolite with 10-ring channel systems, being rather similar to the industrially most frequently employed ZSM-5. The size of the channels of TNU-9 is 0.52 nm × 0.60 nm and 0.51 nm × 0.55 nm, thus a slightly larger zeolite compared with ZSM-5 [41]. A recent diffraction analysis coming as a seminal breakthrough describes the structure solution of a material, TNU-9, that has the greatest number of unique symmetry tetrahedral atoms in the structure (22) of any material solved to date [42].

In this work, the catalytic activity of a novel zeolite TNU-9 possessing 10-10-10-ring system is compared with SSZ-33, ZSM-5 and mordenite in benzene ethylation. Although there are many studies on ethylation of benzene with ethanol over ZSM-5 and mordenite-based catalyst, while a few have been reported over SSZ-33 and none over TNU-9-based catalyst. Most of them are related to catalyst development and elucidation of reaction mechanism. To our knowledge, the kinetic study over TNU-9, SSZ-33 and mordenite-based catalyst in the ethylation of benzene with ethanol has not been reported in the open literature and has not been carried out in a riser simulator. A simplified kinetic model which describes the reaction under the present conditions will be developed. The proposed model will be tested with the obtained experimental data and the model parameters estimated using nonlinear regression analysis.

2. Experimental

2.1. Preparation of catalysts

The uncalcined proton form of mordenite (H-mordenite) zeolite (HSZ-690HOA) used in this work was obtained from Tosoh Chemicals, Japan. The mordenite has silica to alumina ratio of 180. An alumina binder (Cataloid AP-3) contains 75.4 wt% alumina, 3.4% acetic acid and water as a balance. The alumina binder was obtained from CCIC Japan. The alumina binder was dispersed in water and stirred for 30 min to produce thick slurry. The zeolite powder was then mixed with alumina slurry to produce a thick paste. The composition of the zeolite-based catalyst in weight ratio is as follows: Mordenite: AP-3 (2:1). The uncalcined proton form of ZSM-5 (CT-405) used in this study was obtained from CATAL, UK. The ZSM-5 has silica to alumina ratio of 30. Similar procedure used for the preparation of the mordenite-based catalyst used in this study was also followed for the preparation of the ZSM-5-based catalyst. The composition of the ZSM-5 zeolite-based catalyst in weight ratio is as follows: ZSM-5: AP-3 (2:1). Zeolite SSZ-33 and TNU-9 and their characterization data (XRD—not provided in the text, SEM, FTIR) used in this study were obtained from J. Heyrovsky Institute of Physical Chemistry, Academy of Science of the Czech Republic, Prague, Czech Republic. Alumina was added to these zeolites (SSZ-33 and TNU-9) adopting the same procedure used for mordenite and ZSM-5-based catalyst.

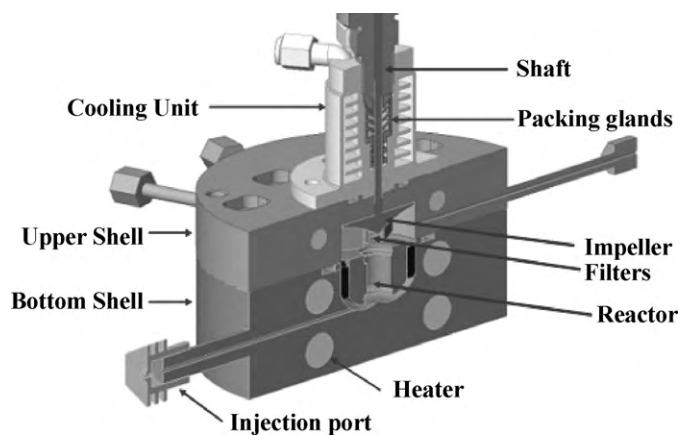


Fig. 1. Schematic diagram of the riser simulator.

2.2. Characterization of catalysts

Surface areas were obtained from N_2 physical adsorption isotherms by applying BET method with Quantachrome AUTO-SORB-1 (model ASI-CT-8). The samples were preheated at 373 K for 3 h in flowing N_2 . Type and concentration of acid sites in all zeolites were determined by adsorption of pyridine as probe molecules followed by FTIR spectroscopy (Nicolet 6700 FTIR) using the self-supported wafers technique. Prior to adsorption, self-supporting zeolite wafers were activated in situ by evacuation at temperature 450 °C over night. Adsorption of pyridine proceeded at 150 °C for 20 min at partial pressure 5 Torr.

The concentrations of Bronsted and Lewis acid sites were calculated from the integral intensities of individual bands characteristic of pyridine on Bronsted acid sites at 1550 cm^{-1} and band of pyridine on Lewis acid sites at 1455 cm^{-1} and molar absorption coefficient [43] of $\varepsilon(B) = 1.67 \pm 0.1\text{ cm} \mu\text{mol}^{-1}$ and $\varepsilon(L) = 2.22 \pm 0.1\text{ cm} \mu\text{mol}^{-1}$, respectively. The infrared spectra of absorbed pyridine on SSZ-33 were recently discussed in detail by Gil et al. [44].

2.3. Reaction procedure

Benzene ethylation was carried out in the riser simulator (see Fig. 1). This reactor is bench scale equipment with internal recycle unit invented by de Lasa [45]. A detailed description of various riser simulator components, sequence of injection and sampling can be found in Kraemer [46]. Catalytic experiments were carried out in the riser simulator with a feed mixture of benzene and ethanol for residence times of 3, 5, 7, 10, 13, 15 and 20 s at temperatures of 250, 275 and 300 °C. Analytical grade (99% purity) pure benzene and ethanol were obtained Sigma–Aldrich. All chemicals were used as received, and no attempt was made to further purify the samples. The feed molar ratio of benzene to ethanol is 1:1. About 800 mg of the fluidizable catalyst particles (60- μm average size) were weighed and loaded into the riser simulator basket. The system was then sealed and tested for any pressure leaks by monitoring the pressure changes in the system. Furthermore, the reactor was heated to the desired reaction temperature. The vacuum box was also heated to $\sim 250\text{ }^\circ\text{C}$ and evacuated to a pressure of $\sim 0.5\text{ psi}$ to prevent any condensation of hydrocarbons inside the box. The heating of the riser simulator was conducted under continuous flow of inert gas (Ar), and it usually takes a few hours until thermal equilibrium is finally attained. Meanwhile, before the initial experimental run, the catalyst was activated for 15 min at 620 °C in a stream of Ar. The temperature controller was set to the desired reaction temperature, and in the same manner, the timer was adjusted to the desired reaction time. At this point, the GC is

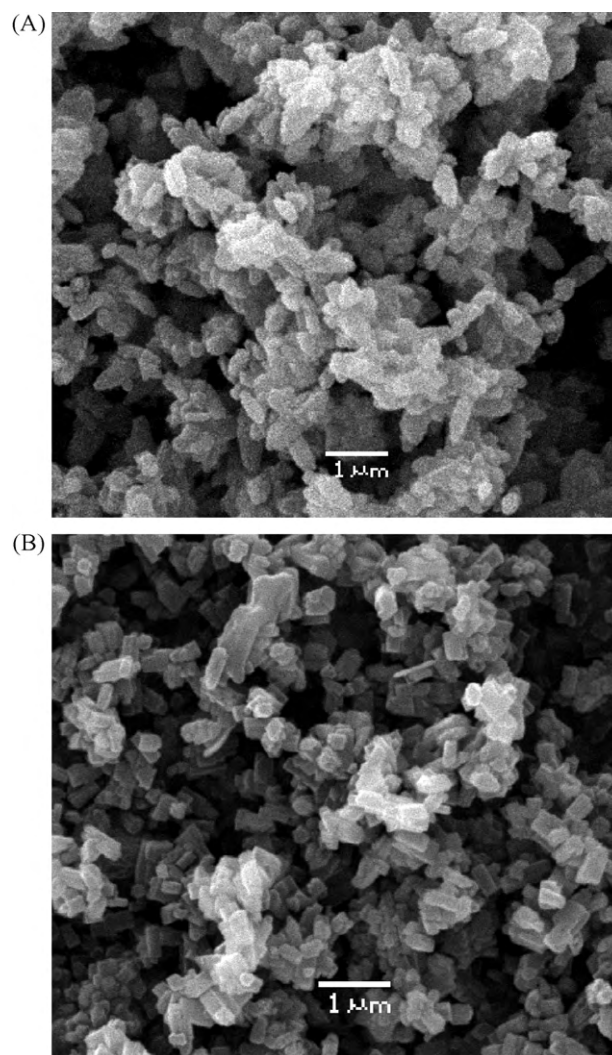


Fig. 2. SEM images of SSZ-33 (A) and TNU-9 (B).

started and set to the desired conditions. Once the reactor and the gas chromatograph have reached the desired operating conditions, 0.162 g of the feedstock was injected directly into the reactor via a loaded syringe. After the reaction, the four-port valve opens immediately, ensuring that the reaction was terminated and the entire product stream was sent on-line to analytical equipment via a pre-heated vacuum box chamber. The products were analyzed in an Agilent 6890N gas chromatograph with a flame ionization detector and a capillary column INNOWAX, 60-m cross-linked methyl silicone with an internal diameter of 0.32 mm. During the course of the investigation, a number of runs were repeated to check for reproducibility in the experimental results, which were found to be excellent. Typical errors were in the range of $\pm 2\%$.

3. Results and discussion

3.1. Characterization of zeolites and catalysts used

X-ray powder patterns of all zeolites under study exhibited good crystallinity and characteristic diffraction lines (not shown here). The shape and size of all zeolites were determined by scanning electron microscopy (Jeol, JSM-5500LV). Fig. 2 shows typical SEM images of zeolites SSZ-33 and TNU-9. The SEM images evidence the absence of impurities including an amorphous one. The crystal sizes of all zeolites used in this present study were between

Table 1
Characteristics of samples used in this work.

| Sample code | Si/Al | Lewis sites (mmol/g) | Bronsted sites (mmol/g) | Lewis sites (%) | Bronsted sites (%) | BET (m ² /g) |
|---------------|-------|----------------------|-------------------------|-----------------|--------------------|-------------------------|
| Parent-ZSM-5 | 30.0 | 0.13 | 0.24 | 35 | 65 | |
| F.C.-ZSM-5 | 20.3 | 0.28 | 0.21 | 57 | 43 | 304 |
| Parent-TNU-9 | 21.9 | 0.15 | 0.43 | 26 | 74 | |
| F.C.-TNU-9 | 19.3 | 0.25 | 0.33 | 43 | 57 | 330 |
| Parent-MOR | 180 | <0.002 | 0.03 | 4 | 96 | |
| F.C.-MOR | 135.9 | 0.12 | 0.03 | 80 | 20 | 441 |
| Parent-SSZ-33 | 18 | 0.43 | 0.30 | 59 | 41 | |
| F.C.-SSZ-33 | 13.6 | 0.48 | 0.18 | 72 | 28 | 448 |
| AP-3 | | 0.64 | 0 | 100 | 0 | 280 |

F.C.—Final Catalyst.

0.3 and 1 μm . Table 1 provides the quantitative evaluation of FTIR spectra of parent zeolites and final catalysts. For application of zeolites in acid catalyzed reactions, the concentration of acid sites (Bronsted and Lewis types) is of utmost importance. The concentration of Bronsted acid sites and all acid sites of all catalysts under study is presented in Table 1. In this case the following sequences were obtained: mordenite < SSZ-33 < ZSM-5 < TNU-9 for Bronsted sites and mordenite < ZSM-5 < TNU-9 < SSZ-33 for all sites. It was observed that addition of alumina binder led to the decrease in Si/Al ratio for all catalysts and to a simultaneous increase in the concentration of Lewis acid sites.

3.2. Ethylation of benzene over mordenite (M-catalyst)

3.2.1. Benzene conversion

The formation of ethylbenzene (EB), diethylbenzene (DEB) and triethylbenzene (TEB) (Table 2) via ethylation of benzene with ethanol was studied over mordenite-based catalyst at 250, 275, and 300 °C for residence times of 3, 5, 7, 10, 13, 15 and 20 s. Benzene conversions of approximately 20.2, 14.5, and 9.7% were achieved at 300, 275 and 250 °C, respectively, for a reaction time of 20 s, as shown in Fig. 3. At all reaction times studied, the maximum benzene conversion was obtained at 300 °C. The experimental results showed that the conversion occurred via ethylation. The major product of the ethylation reaction over M-catalyst is ethylbenzene.

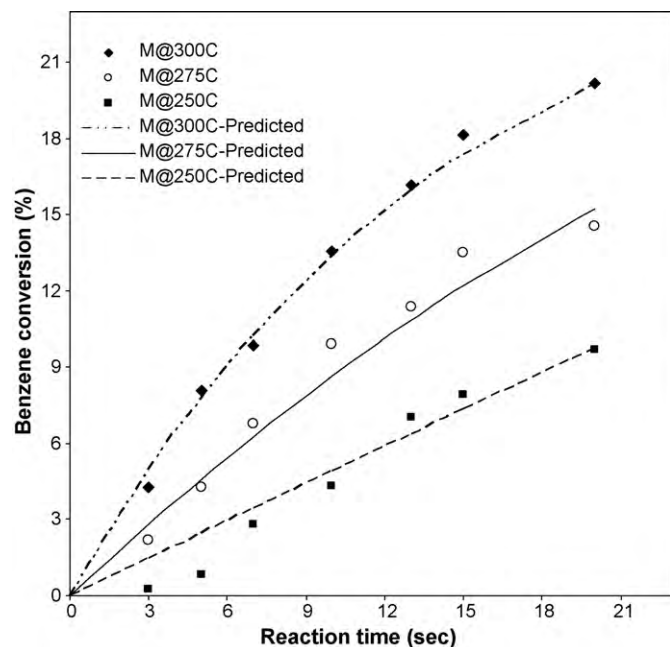


Fig. 3. Variation of benzene conversion with time-on-stream achieved over mordenite-based catalyst at 250 (■), 275 (○) and 300 °C (◆) for catalyst/feed = 5.

A maximum EB yield of ~10.2% was obtained at 300 °C at a benzene conversion of 20.2% for a reaction time of 20 s. Diethylbenzene was also observed in significant amount in the ethylation reaction over mordenite-based catalyst. The highest triethylbenzene (TEB) yield of ~3.0% was achieved at 300 °C at 20.2% benzene conversion. The product distribution is partially reproduced in Table 2. Formation of ethylbenzene represents the primary ethylation step, while the ethylation reaction of EB with ethanol represents the secondary ethylation reaction. A tertiary ethylation reaction was also observed in this reaction, which led to the formation of triethylbenzene (TEB). The formation of TEB is as a result of the channel opening of mordenite that is large enough for the alkylation reaction. The channel opening provides larger reaction volume enabling consecutive reactions of DEB to proceed.

3.2.2. Ethylbenzene and DEB Yield

The yield of ethylbenzene was found to increase with both temperature and time, up to a maximum of ~10.2% at 300 °C for a reaction time of 20 s. This corresponds to an ethylbenzene selectivity of ~50.7%. Cracking of ethylbenzene to produce toluene was not observed in this reaction compared to the pronounced EB cracking reported in our recent publication [38] over USY-zeolite-based catalyst.

Similar to ethylbenzene yield, diethylbenzene yield was noticed to increase with both time and temperature. A maximum of ~6.3% yield of DEB was obtained at 300 °C at a benzene conversion of ~20.2% for a reaction time of 20 s. The experimental results showed that m-DEB was found to be in significant amount more than other DEB isomers detected in this ethylation reaction. The thermodynamic equilibrium mixture of diethylbenzenes (para: meta: ortho = 30:54:16) reported by Kaeding [47] and Halgeri [48] was compared with the DEB isomers obtained under this present study. It can be observed from Table 2 that, for all the reaction conditions studied; p/o ratio was found to be between 1.5 and 3.2, which compared favorably well with the thermodynamic equilibrium values given by previous researchers.

3.3. Ethylation of benzene over ZSM-5 (Z-catalyst)

3.3.1. Benzene conversion

The main products obtained from the ethylation reaction of benzene with ethanol over ZSM-5-based catalyst were ethylbenzene and diethylbenzene (Table 3). Small amount of toluene and gaseous hydrocarbon was also noticed from the reaction products. A maximum benzene conversion of ~21.7% was obtained at 300 °C for a reaction of 20 s. The conversion of benzene was observed to increase with reaction temperature and time, as shown in Fig. 4. This is in conformity with observation made by Odedairo and Al-Khattaf [32] during the ethylation of benzene over ZSM-5-based catalyst, in which kaolin and alumina were used as the filler and silica sol was used as the binder. About 2.2–8.6% of toluene was also noticed in this ethylation reaction over ZSM-5-based catalyst,

Table 2
Product distribution (wt%) at various reaction conditions for the ethylation of benzene over mordenite-based catalyst.

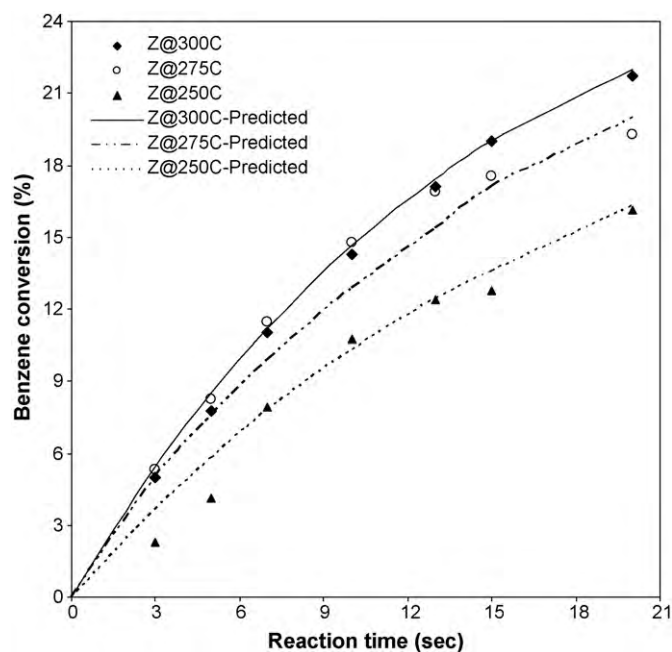
| Temperature (°C) | Time (s) | Benzene conv (%) | EB | Toluene | Gases | m-DEB | p-DEB | o-DEB | Total DEB | TEB |
|------------------|----------|------------------|-------|---------|-------|-------|-------|-------|-----------|------|
| 250 | 5 | 0.81 | 0.49 | – | – | 0.08 | 0.03 | 0.02 | 0.13 | 0.19 |
| | 10 | 4.33 | 2.37 | – | 0.09 | 0.49 | 0.27 | 0.13 | 0.89 | 0.98 |
| | 15 | 7.92 | 4.05 | – | 0.23 | 1.08 | 0.44 | 0.22 | 1.74 | 1.90 |
| | 20 | 9.72 | 4.83 | – | 0.26 | 1.44 | 0.55 | 0.28 | 2.27 | 2.36 |
| 275 | 5 | 4.30 | 2.51 | – | – | 0.59 | 0.22 | 0.12 | 0.93 | 0.86 |
| | 10 | 9.92 | 5.24 | – | 0.20 | 1.59 | 0.65 | 0.26 | 2.50 | 1.98 |
| | 15 | 13.51 | 6.67 | – | 0.36 | 2.28 | 0.98 | 0.36 | 3.62 | 2.86 |
| | 20 | 14.53 | 7.26 | – | 0.36 | 2.55 | 1.12 | 0.37 | 4.04 | 2.87 |
| 300 | 5 | 8.07 | 4.61 | – | 0.12 | 1.40 | 0.63 | 0.21 | 2.24 | 1.10 |
| | 10 | 13.55 | 7.07 | – | 0.25 | 2.52 | 1.13 | 0.36 | 4.01 | 2.22 |
| | 15 | 18.16 | 9.30 | 0.18 | 0.45 | 3.47 | 1.57 | 0.49 | 5.53 | 2.70 |
| | 20 | 20.16 | 10.23 | 0.25 | 0.46 | 3.93 | 1.78 | 0.55 | 6.26 | 2.96 |

T = 250–300 °C and catalyst/feed = 5.

Table 3
Product distribution (wt%) at various reaction conditions for the ethylation of benzene over ZSM-5-based catalyst.

| Temperature (°C) | Time (s) | Benzene Conv (%) | EB | Toluene | Gases | m-DEB | p-DEB | o-DEB | Total DEB |
|------------------|----------|------------------|-------|---------|-------|-------|-------|-------|-----------|
| 250 | 5 | 4.13 | 3.01 | 0.09 | 0.08 | 0.50 | 0.43 | 0.03 | 0.95 |
| | 10 | 10.76 | 7.55 | 0.34 | 0.25 | 1.27 | 1.25 | 0.10 | 2.62 |
| | 15 | 12.74 | 8.90 | 0.48 | 0.30 | 1.49 | 1.46 | 0.11 | 3.06 |
| | 20 | 16.10 | 11.23 | 0.70 | 0.34 | 1.94 | 1.72 | 0.17 | 3.83 |
| 275 | 5 | 8.24 | 5.96 | 0.32 | 0.20 | 0.93 | 0.75 | 0.08 | 1.76 |
| | 10 | 14.75 | 10.63 | 0.84 | 0.34 | 1.54 | 1.25 | 0.15 | 2.94 |
| | 15 | 17.54 | 12.21 | 0.87 | 0.37 | 2.13 | 1.78 | 0.18 | 4.09 |
| | 20 | 19.29 | 13.29 | 1.12 | 0.52 | 2.33 | 1.81 | 0.22 | 4.36 |
| 300 | 5 | 7.78 | 5.62 | 0.54 | 0.26 | 0.73 | 0.55 | 0.08 | 1.36 |
| | 10 | 14.28 | 10.12 | 1.24 | 0.39 | 1.36 | 1.01 | 0.15 | 2.53 |
| | 15 | 19.02 | 13.20 | 1.42 | 0.68 | 2.06 | 1.42 | 0.23 | 3.71 |
| | 20 | 21.70 | 14.94 | 1.88 | 0.88 | 2.29 | 1.44 | 0.27 | 4.00 |

T = 250–300 °C and catalyst/feed = 5.

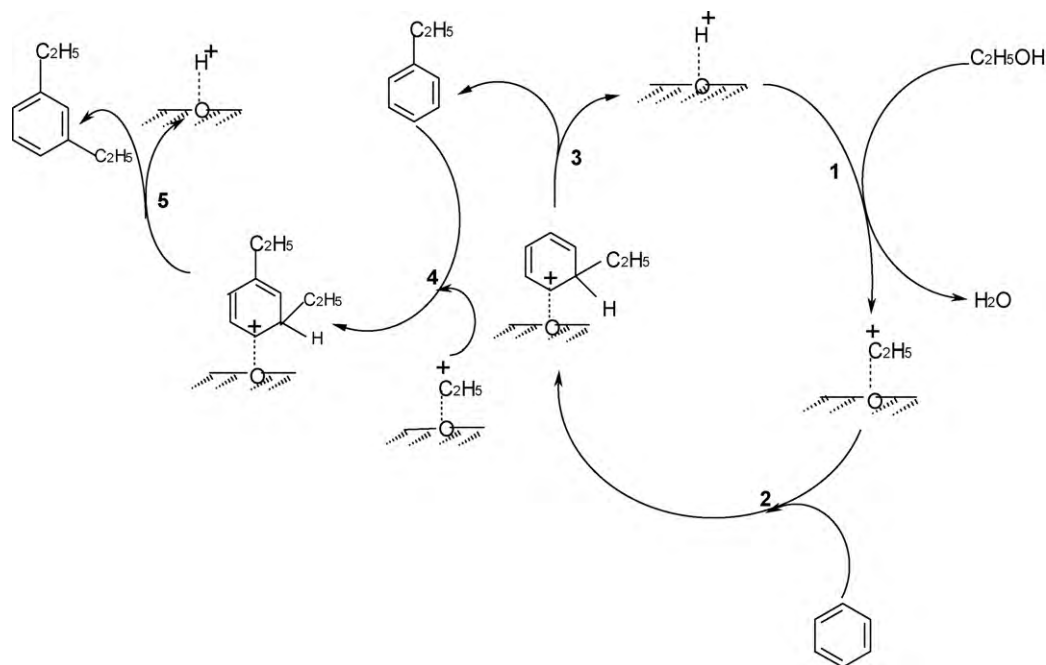
**Fig. 4.** Variation of benzene conversion with time-on-stream achieved over ZSM-5-based catalyst at 250 (▲), 275 (○) and 300 °C (◆) for catalyst/feed = 5.

as compared with a negligible amount reported in our recent publication over another catalyst which was also based on ZSM-5 [32]. The small amount of toluene observed in this ethylation reaction is due to the higher acidity of the ZSM-5 used in this present study as compared with the one previously reported, which was of a lower acidity (0.23 mmol/g). The noticeable amount of toluene observed at the higher temperatures, is probably formed from the cracking of ethylbenzene.

A possible mechanism to represent the ethylation of benzene with ethanol over ZSM-5 is illustrated in Scheme 1. Surface proton attacks ethanol to form water and surface ethyl cation (ethoxy cation). An ethyl cation attacks benzene molecule to form protonated ethylbenzene on the surface. The protonated ethylbenzene returns a proton to the surface and forms ethylbenzene. Thereafter, surface ethyl cation (ethoxy cation) attacks ethylbenzene ring carbon atom at ortho, meta or para position atom to form a surface protonated diethylbenzene. The surface protonated diethylbenzene returns a proton to the surface and forms diethylbenzene.

3.3.2. Ethylbenzene and DEB Yield

The yield of ethylbenzene increased with reaction time and temperature, up to ~14.9% at 300 °C, for a reaction time of 20 s. EB yield of 13.3 and 11.2% was also obtained at 275 °C and 250 °C, respectively. An optimum yield of ~4.4% of DEB was noticed at 275 °C for a reaction time of 20 s. As temperature was further increased to 300 °C, a slight decrease in DEB yield was observed to a value of ~4.0%. In the ethylation reaction of benzene with ethanol over ZSM-



Scheme 1. Proposed overall reaction scheme during benzene ethylation.

5-based catalyst, the formation of para-isomers can be expected to proceed almost entirely in the zeolite channel system, while the formation of meta- and ortho-isomers proceeds on the external surface. The p/o ratio obtained from the ethylation of benzene with ethanol over ZSM-5-based catalyst was found to range between ~5.3 and 14.3. This value was noticed to be far above the thermodynamic equilibrium value given by Kaeding [47] and Halgeri [48].

It is of paramount importance to note that triethylbenzene was not formed in the ethylation reaction over ZSM-based catalyst. Even if the alkylation product (TEB) is formed in the large channel intersections, its chances to leave the channel would be very small. This also goes to ascertain the fact that zeolite with 10 rings usually exhibits restricted transition-state and product shape selectivity being particularly important in para-selective reactions such as toluene disproportionation, xylene isomerization, and toluene alkylation with methanol, ethylene/ethanol and propylene/propanol [49–56].

3.4. Ethylation of benzene over SSZ-33

Ethylbenzene and toluene were observed to be the main products obtained from the ethylation of benzene with ethanol over SSZ-33. Benzene conversion was found to increase with reaction time for all temperatures studied, reaching maximum of ~27% at 275 °C. Toluene selectivity shows a high dependence on reaction temperature over SSZ-33 catalyst, showing a toluene selectivity rise from ~25 to 43% and then to ~54% for temperatures of 250, 275, and 300 °C, for 20 s reaction time, respectively. The selectivity of toluene increased with increase in temperature. The significant increase in the selectivity of toluene indicates that the ethylbenzene formed undergoes cracking at higher temperature. Gao et al. [30] gave similar explanation when traces of toluene were found in the alkylation of benzene with ethanol over ZSM-5-based catalyst. They attributed the formation of toluene to the cracking of ethylbenzene over Bronsted acid sites.

Ethylbenzene selectivity decreased steadily with increase in temperature over SSZ-33-based catalyst to minimum of ~34% at 300 °C for a reaction time of 20 s. It is evident from Table 4 that

as temperature was increased from 250 to 300 °C; more toluene was formed due to ethylbenzene cracking, leading to a decrease in the selectivity of ethylbenzene at higher temperature. Negligible amount of DEB was noticed at 250 °C, while no DEB was formed at the higher temperatures.

According to the product distribution over SSZ-33-based catalyst, a possible reaction mechanism representing the reaction of benzene with ethanol over SSZ-33 is given by Scheme 2. Surface proton attacks ethanol to form water and surface ethyl cation (ethoxy cation). An ethyl cation attacks benzene molecule to form protonated ethylbenzene on the surface. The protonated ethylbenzene returns a proton to the surface and forms ethylbenzene. Surface proton reacts with ethylbenzene to form a carbonium ion I. These carbonium ion I form surface methyl cation (methoxy cation) and toluene. The surface methyl cation formed reacts with benzene molecule to form protonated toluene. The protonated toluene returns a proton to the surface and forms toluene.

3.5. Ethylation of benzene over TNU-9

Table 5 shows the product distribution of TNU-9 catalyst in the ethylation of benzene with ethanol at variable temperatures of 250, 275 and 300 °C. EB, toluene, DEB and gaseous hydrocarbons were found in the ethylation reaction. Benzene conversion increased with reaction time, up to a maximum of ~25.0% at 300 °C.

Ethylation was noticed to be the major reaction, while at elevated temperatures the cracking reaction is also important. Cracking reaction of EB and DEB was observed at elevated temperatures, leading to increased cracking product (toluene) at elevated temperatures. The ethylation and cracking reaction noticed over TNU-9-based catalyst in the ethylation reaction of benzene with ethanol is similar to the reactions observed during benzene ethylation with ethanol over USY catalyst reported in our recent publication [38]. Both toluene and EB selectivity shows a high dependence on temperature over TNU-9 catalyst. The selectivity of toluene increased with increase in temperature, while the selectivity of ethylbenzene and DEB decreased with increase in temperature.

Table 4
Product distribution (wt%) at various reaction conditions for the ethylation of benzene over SSZ-33 catalyst.

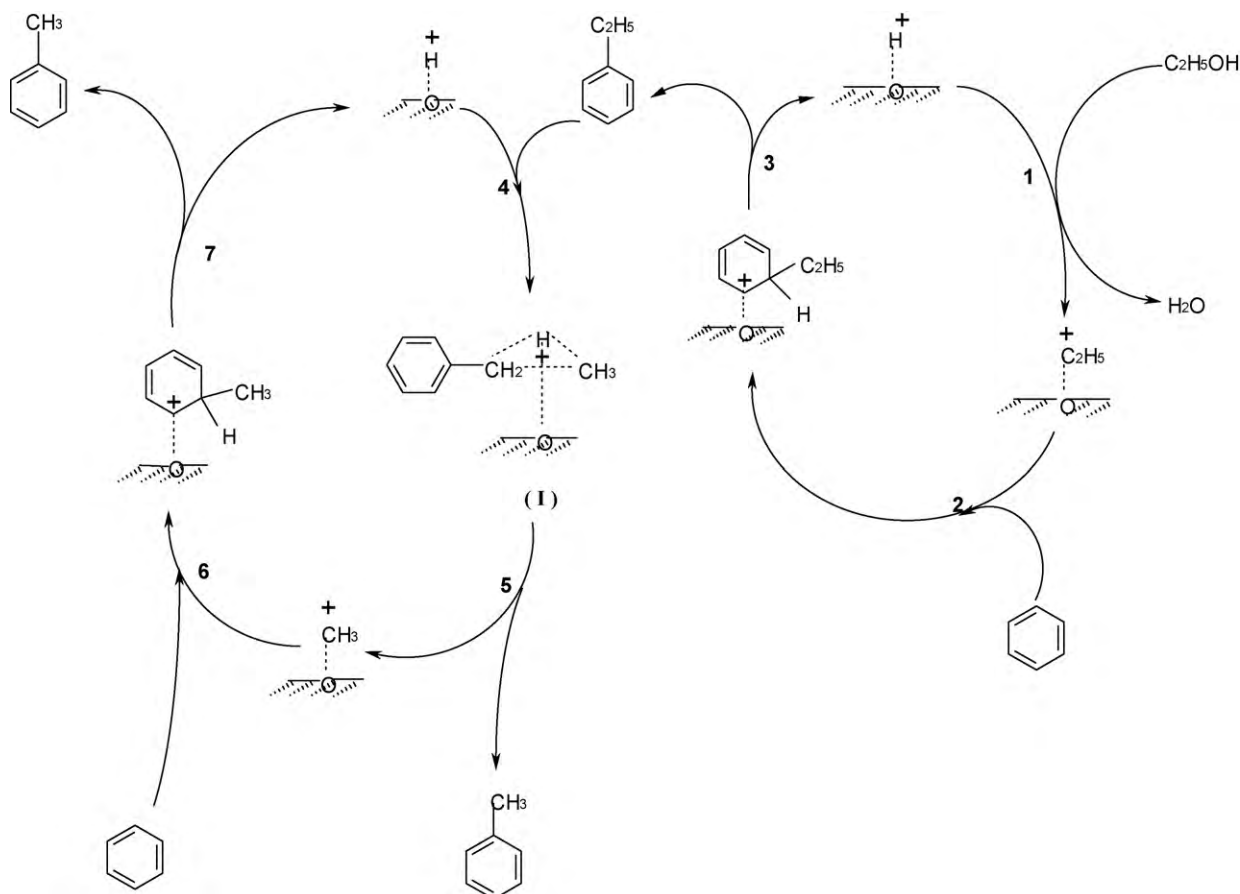
| Temperature (°C) | Time (s) | Benzene conv (%) | EB | Toluene | Gases | m-DEB | p-DEB | o-DEB | Total DEB |
|------------------|----------|------------------|-------|---------|-------|-------|-------|-------|-----------|
| 250 | 5 | 12.08 | 7.81 | 2.01 | 1.33 | 0.56 | 0.29 | 0.08 | 0.93 |
| | 10 | 18.86 | 12.93 | 2.86 | 1.65 | 0.88 | 0.41 | 0.12 | 1.42 |
| | 15 | 24.17 | 15.41 | 4.95 | 2.11 | 1.04 | 0.53 | 0.13 | 1.70 |
| | 20 | 25.28 | 14.94 | 6.26 | 2.32 | 1.04 | 0.58 | 0.14 | 1.76 |
| 275 | 5 | 12.85 | 8.03 | 3.25 | 1.57 | – | – | – | – |
| | 10 | 18.57 | 10.01 | 6.39 | 2.17 | – | – | – | – |
| | 15 | 25.43 | 11.85 | 10.76 | 2.82 | – | – | – | – |
| | 20 | 27.24 | 12.35 | 11.75 | 3.14 | – | – | – | – |
| 300 | 5 | 16.26 | 6.76 | 7.39 | 2.11 | – | – | – | – |
| | 10 | 23.85 | 7.97 | 13.34 | 2.54 | – | – | – | – |
| | 15 | 24.97 | 8.25 | 13.89 | 2.83 | – | – | – | – |
| | 20 | 26.38 | 8.87 | 14.18 | 3.33 | – | – | – | – |

T = 250–300 °C and catalyst/feed = 5.

3.6. Comparison of catalysts in the ethylation of benzene with ethanol

Fig. 5 provides time-on-stream dependence of benzene conversion at 300 °C over zeolite-based catalysts prepared from ZSM-5, TNU-9, SSZ-33 and mordenite materials. It is evident from this figure that, over all the catalysts studied, benzene conversion increases as expected with increase in reaction time (5–20 s). The conversion of benzene in the ethylation reaction of benzene with ethanol carried out at 300 °C for a contact time of 20 s, follows the order: SSZ-33 (26%) > TNU-9 (25%) > ZSM-5 (22%) > mordenite (20%).

Based on the comparison of the role of structure of the zeolites on benzene conversion in ethylation reaction of benzene with ethanol, it can be inferred that more open structure of SSZ-33-based catalyst (12-12-10-ring), which has been known to combine both large and medium pore channels [8], allows a higher reaction rate and faster diffusion of both reactants and products in comparison with the medium pore (10-ring) ZSM-5 and TNU-9 zeolite. Similar explanation was given during toluene disproportionation reaction over zeolite-based catalysts when an increase in toluene conversion was observed [57]. They attributed the increase in conversion to the increase in the size of channels from medium to large pore zeolites. The above trend in which the lowest benzene



Scheme 2. Proposed reaction scheme for toluene formation during benzene ethylation reaction with ethanol.

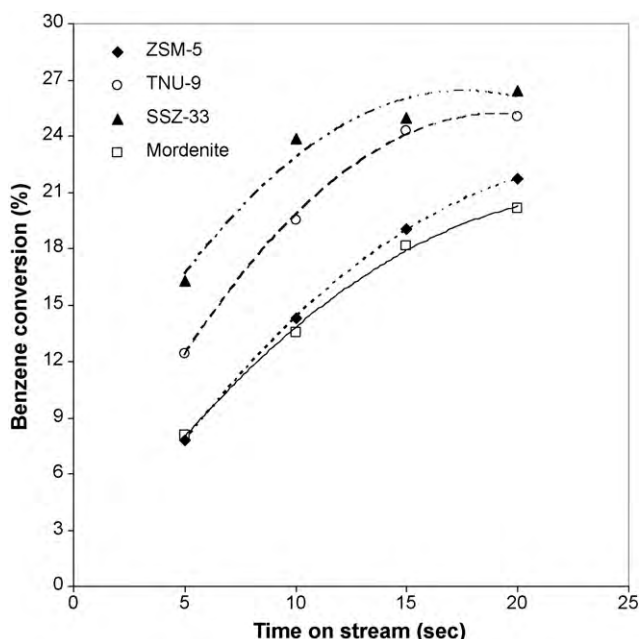


Fig. 5. Time-on-stream dependence of benzene conversion in benzene ethylation over ZSM-5 (◆), TNU-9 (○), SSZ-33 (▲) and mordenite (□) at 300 °C for catalyst/feed = 5.

conversion was noticed over mordenite-based catalyst is expected since mordenite, with a set of 12-ring channels interconnected by another set of 8-ring cross channels, in which the cross channels are sufficiently small that they do not provide a means for transport of molecules between adjacent passageways [58]. It was also pointed out that with respect to hydrocarbons, the structure is effectively one-dimensional and may be regarded as an array of parallel, noninterconnecting channels. Similarly, it has also been reported by Chen et al. [59] that in mordenite, the eight-membered ring channels with aperture size of $2.6 \text{ \AA} \times 5.7 \text{ \AA}$ which crosses the 12-membered ring channels are actually windows rather than channels and they found it not readily accessible to chromium ions during metal exchange. Abdullah et al. [60] reported that such narrow apertures make it difficult for benzene molecule to diffuse. In addition, Zilkova et al. [8] found the 8-ring channels of mordenite inaccessible for toluene as well.

The calculated concentrations of Bronsted and Lewis sites are presented in Table 1. Individual zeolite-based catalysts under study vary in Si/Al ratio as well as in the concentrations of Bronsted

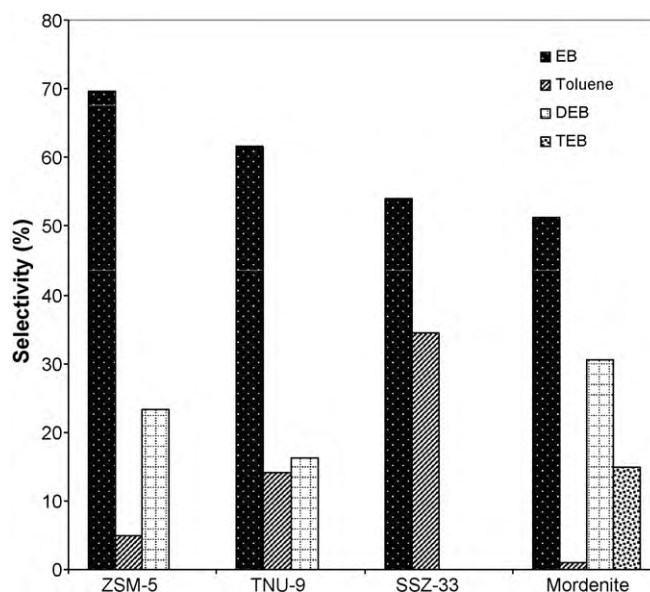


Fig. 6. Product selectivity of benzene ethylation over the different catalysts at 18% benzene conversion (catalyst/feed = 5, reaction temperature: 250, 275 and 300 °C).

and Lewis acid sites. The order of the concentrations of Bronsted acid sites, calculated for the different catalysts, is mordenite < SSZ-33 < ZSM-5 < TNU-9. If the total amount of acid sites (Bronsted plus Lewis) is taken into account, the order is slightly different: mordenite < ZSM-5 < TNU-9 < SSZ-33, mainly because of the high concentration of Lewis sites in zeolite SSZ-33. In both cases, mordenite gave the least amount of acid sites for both the Bronsted acid sites as well as in all acid sites (Bronsted plus Lewis). Mordenite, possessing the lowest amount of acid sites, gave the lowest benzene conversion as compared with other zeolite-based catalysts. Catalyst based on ZSM-5 showed comparable benzene conversions with the one noticed over mordenite-based catalyst. The lowest benzene conversion over mordenite- and ZSM-5-based catalyst is due to larger pores of mordenite with low amount of acid sites providing similar results as ZSM-5 with smaller channels but higher concentration of acid sites. Therefore, in the case of mordenite, its unique channel architecture as well as low amount acid sites accounts for the low benzene conversion noticed over this zeolite-based catalyst.

The product selectivity during the ethylation of benzene with ethanol over ZSM-5, TNU-9, SSZ-33 and mordenite-based catalyst is compared in Fig. 6 at constant conversion level of 18% at 250,

Table 5
Product distribution (wt%) at various reaction conditions for the ethylation of benzene over TNU-9 catalyst.

| Temperature (°C) | Time (s) | Benzene Conv (%) | EB | Toluene | Gases | m-DEB | p-DEB | o-DEB | Total DEB |
|------------------|----------|------------------|-------|---------|-------|-------|-------|-------|-----------|
| 250 | 5 | 10.92 | 6.90 | 1.43 | 0.81 | 1.09 | 0.58 | 0.11 | 0.95 |
| | 10 | 17.65 | 10.89 | 2.49 | 1.39 | 1.79 | 0.97 | 0.15 | 2.88 |
| | 15 | 23.78 | 14.84 | 3.37 | 1.63 | 2.44 | 1.27 | 0.23 | 3.94 |
| | 20 | 25.01 | 15.19 | 3.95 | 1.73 | 2.57 | 1.34 | 0.23 | 4.14 |
| 275 | 5 | 12.19 | 7.46 | 1.87 | 0.85 | 1.23 | 0.65 | 0.13 | 2.01 |
| | 10 | 20.94 | 12.20 | 4.02 | 2.10 | 1.60 | 0.84 | 0.18 | 2.62 |
| | 15 | 24.20 | 13.55 | 5.07 | 2.23 | 2.08 | 1.07 | 0.20 | 3.35 |
| | 20 | 24.58 | 13.60 | 5.29 | 2.25 | 2.12 | 1.10 | 0.22 | 3.44 |
| 300 | 5 | 12.41 | 6.09 | 2.91 | 1.38 | 1.19 | 0.45 | 0.10 | 1.38 |
| | 10 | 19.53 | 10.09 | 5.11 | 1.88 | 1.49 | 0.80 | 0.15 | 2.45 |
| | 15 | 24.31 | 11.54 | 7.64 | 2.16 | 1.72 | 1.07 | 0.18 | 2.97 |
| | 20 | 25.06 | 11.78 | 7.83 | 2.26 | 1.97 | 1.01 | 0.21 | 3.19 |

T = 250–300 °C and catalyst/feed = 5.

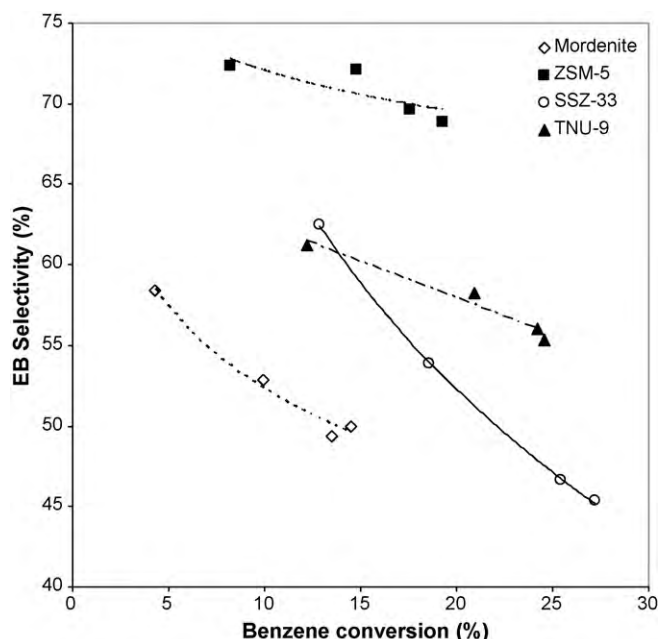


Fig. 7. Effect of benzene conversion on ethylbenzene selectivity (catalyst/feed = 5, reaction temperature 275 °C).

275 and 300 °C reaction temperatures. The results show that ethylbenzene (EB) is obtained as the most predominant product over all the catalysts. The formation of EB with high selectivity over all the catalysts might be due to its free diffusion without steric hindrance through the pores of the catalysts. Catalyst based on ZSM-5 gave the highest EB selectivity of ~70%, and mordenite-based catalyst gave the lowest with an EB selectivity of ~51%. SSZ-33 gave the highest toluene selectivity of ~34% among all the catalysts studied, at a constant benzene conversion of 18%. It is worth mentioning that DEB was not observed over SSZ-33 catalyst at all conversion levels, except at 250 °C, which gave negligible amount of DEB. In contrast, a significant amount of DEB was obtained over mordenite as compared to SSZ-33 catalyst. Mordenite, however, gave the lowest selectivity towards toluene, particularly at lower reaction temperatures.

With respect to the ethylation products, it can be seen from Fig. 6 that TNU-9 behaves like the 10-ring ZSM-5 for EB and DEB selectivity, while SSZ-33 shows no selectivity towards DEB. The effect of benzene conversion on ethylbenzene selectivity at 275 °C over all zeolite-based catalysts under study is given in Fig. 7. EB selectivity over SSZ-33, mordenite and TNU-9-based catalyst shows a high dependence on benzene conversion and was noticed to decrease as benzene conversion increases. Ethylbenzene selectivity over ZSM-5-based catalyst on the other hand, shows a moderate dependence on benzene conversion. Fig. 8a shows the effect of conversion of benzene on diethylbenzene selectivity at 275 °C. It can be noted that the diethylbenzene selectivity depends on both type of catalyst and temperature (Fig. 8a and b). On the other hand, in all cases mordenite has shown higher selectivity, followed by ZSM-5 and TNU-9, while the SSZ-33 has shown no selectivity of diethylbenzene at this particular temperature. Both ZSM-5 and TNU-9 catalysts have shown the maximum selectivity at 250 °C, after which an obvious drop can be seen. In the case of mordenite, diethylbenzene selectivity increased with conversion and reaction temperature in which the maximum selectivity was obtained at 300 °C. This trend is clear in Fig. 8b, where the comparison is performed for 20 s reaction time.

The ratio of toluene to ethylbenzene has been plotted versus benzene conversion for its ethylation reaction over mordenite-, ZSM-5-, SSZ-33- and TNU-9-based catalysts as shown in Fig. 9a. The

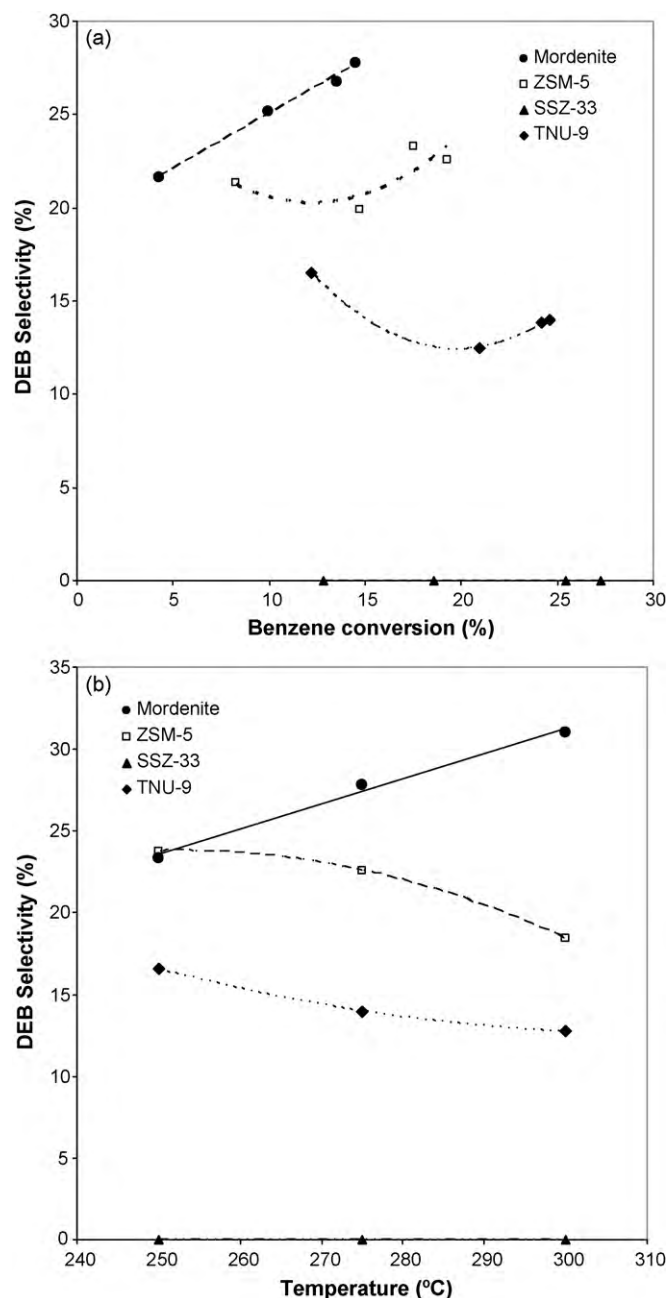


Fig. 8. (a) Effect of benzene conversion on diethylbenzene selectivity at 275 °C on catalysts (●) mordenite, (□) ZSM-5, (▲) SSZ-33 and (◆) TNU-9. (b) Benzene ethylation: effect of temperature on diethylbenzene selectivity at reaction time of 20 s on (●) mordenite, (□) ZSM-5, (▲) SSZ-33 and (◆) TNU-9.

toluene/EB ratios at 250 °C were found in the order: MOR < ZSM-5 < TNU-9 < SSZ-33 (Fig. 9a). The above trend is completely reverse to the trend which was noticed in the case of DEB selectivity with benzene conversion in the sense that, in all cases, SSZ-33 gave the lowest selectivity. This trend confirms that little or no cracking of ethylbenzene occurred over mordenite-based catalyst, which accounts for the high DEB selectivity noticed over mordenite catalyst, since the production of DEB is at the expense of ethylbenzene conversion to DEB (second ethylation step). The ratio of toluene/EB is between 0 and 0.42 at 250 °C for the benzene ethylation over all the zeolite-based catalysts under study. However, as temperature increases, the ratio increased from 0.42 to about 1.68 (i.e., four times more) as shown in Fig. 9b. Cracking of the ethylation product (EB) is responsible for the higher toluene-to-EB ratio at higher tempera-

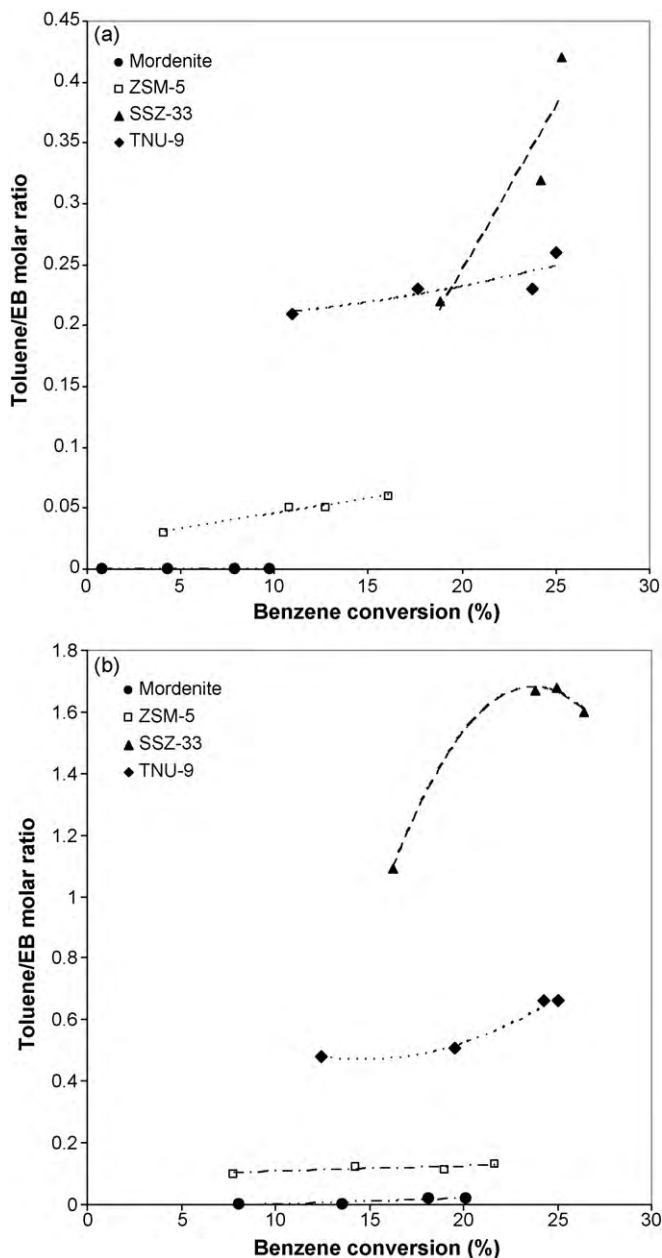


Fig. 9. Toluene/EB ratio with benzene conversion at (a) 250 °C and (b) 300 °C on catalysts (●) mordenite, (□) ZSM-5, (▲) SSZ-33 and (◆) TNU-9.

tures. The effect of total acid sites on toluene formation at constant conversion level of 20% at 300 °C over all the zeolite-based catalysts under study is given in Fig. 10. The yield of toluene increased with increase in total acid sites. It was observed that a maximum toluene yield of about 10.3% was obtained at 300 °C over SSZ-33-based catalyst at 20% benzene conversion. Therefore, to reduce cracking of ethylbenzene in the ethylation reaction over all the zeolite-based catalysts, the total acid sites need to be balanced.

It is a well-established fact that the formation of dialkylbenzenes provides vital knowledge on the structure and acidity of zeolite catalysts [8]. From product diffusion shape selectivity effects, it is expected that the p/o ratio of the DEB isomers would be higher in medium pore ZSM-5-based catalyst than in the large pore zeolite. Within the distribution of isomers in the DEB, ZSM-5 showed the highest p/o ratio of ~9.9 at constant conversion level of 18%, while the lowest was noticed over SSZ-33. In conclusion, according to the results presented above, ZSM-5-based catalyst shows a

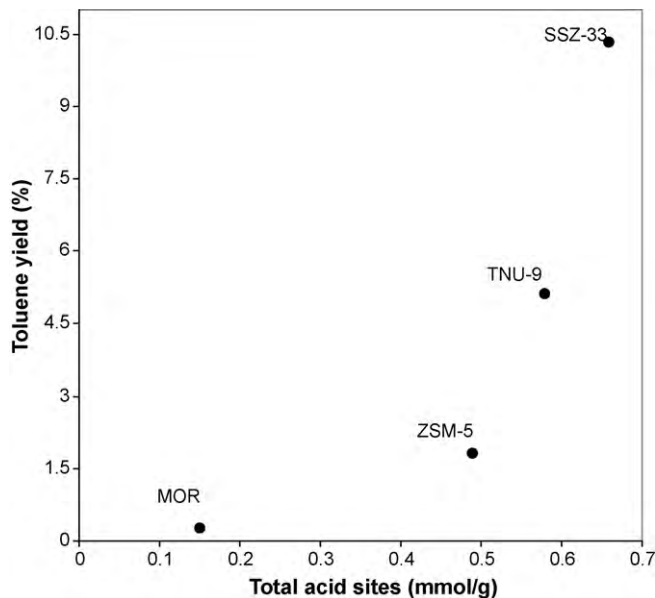


Fig. 10. Effect of total acid sites on toluene formation at 300 °C at 20% benzene conversion.

slightly higher selectivity towards the formation of EB than TNU-9 and a much higher EB selectivity than SSZ-33 and mordenite-based catalyst.

4. Kinetic modeling

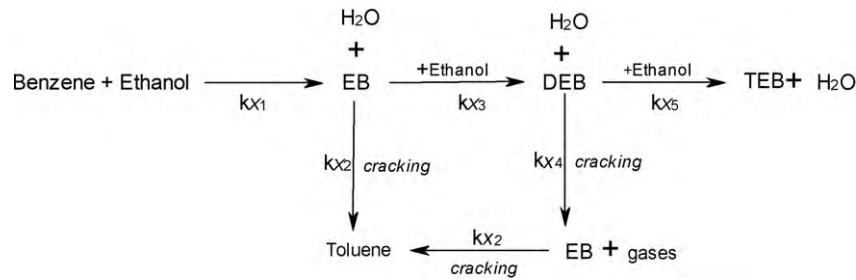
In this section, a comprehensive universal kinetic model for benzene ethylation over all the zeolite-based catalysts under study was developed. To develop a suitable kinetic model representing the overall ethylation of benzene with ethanol, we propose the reaction network shown in Scheme 3.

4.1. Model development for ethylation reaction over mordenite-based catalyst

Based on the product distribution observed in the ethylation reaction over mordenite-based catalyst (Table 2), a suitable kinetic model representing the ethylation reaction can be developed. Since toluene was not observed as one of the products in the ethylation reaction over mordenite-based catalyst, the cracking of ethylbenzene as well as the cracking of diethylbenzene can therefore be neglected.

It should be noted that the following assumptions were made in deriving the reaction network:

1. An irreversible reaction path is assumed for the ethylation reactions. Similar assumption was made by Sridevi et al. [61].
2. Catalysts deactivation is assumed to be a function of reactant conversion (RC). A single deactivation function is defined for all the reactions taking place.
3. Isothermal operating conditions can also be assumed given the design of the riser simulator unit and the relatively small amount of reacting species [45]. This is justified by the negligible temperature change observed during the reactions.
4. A pseudo-first-order reaction kinetic for all species involved in the reactions.
5. Negligible thermal conversion.
6. A single effectiveness factor was considered for benzene, ethylbenzene and triethylbenzene.
7. The effectiveness factor η was taken to be unity. This assumption was made based on the fact that p-xylene formed by catalytic



Scheme 3.

reaction can easily escape via the pores of ZSM-5 [62] comparing mordenite with a larger pore opening; no diffusion restriction is expected in this reaction.

Therefore, k_{x2} and $k_{x4} \approx 0$, (where $x = m$ in the case of mordenite). The following set of species balances and catalytic reactions can be written:

Rate of disappearance of benzene:

$$-\frac{V}{W_c} \frac{dC_B}{dt} = \eta k_{m1} C_B C_E \varphi \quad (1)$$

Rate of formation of ethylbenzene:

$$\frac{V}{W_c} \frac{dC_{EB}}{dt} = (\eta k_{m1} C_B C_E - \eta k_{m3} C_{EB} C_E) \varphi \quad (2)$$

Rate of diethylbenzene formation:

$$\frac{V}{W_c} \frac{dC_{DEB}}{dt} = (\eta k_{m3} C_{EB} C_E - \eta k_{m5} C_{DEB} C_E) \varphi \quad (3)$$

Rate of triethylbenzene formation:

$$\frac{V}{W_c} \frac{dC_{TEB}}{dt} = \eta k_{m5} C_{DEB} C_E \varphi, \quad (4)$$

where C_B is the benzene concentration, C_{EB} is the concentration of ethylbenzene, C_{DEB} is the concentration of diethylbenzene, C_{TEB} is the concentration of triethylbenzene in the riser simulator, V is the volume of the riser (45 cm³), W_c is the mass of the catalyst (0.81 g of catalyst), t is the time (s), φ is the apparent deactivation function, η = an effectiveness factor and k is the rate constant (cm³/(g of catalyst.s)). By definition the molar concentration, C_x , of every species in the system can be related to its mass fraction, y_x (measurable from GC), by the following relation:

$$C_x = \frac{y_x W_{hc}}{V MW_x}, \quad (5)$$

where W_{hc} is the weight of feedstock injected into the reactor, MW_x is the molecular weight of specie x in the system, V is the volume of riser simulator.

Regarding catalyst deactivation, as deactivation functions can be expressed in terms of the catalyst time-on-stream [$\varphi = \exp(-\alpha t)$], deactivation can also be related to the progress of the reaction [63]. The deactivation function based on time-on-stream was initially suggested by Voorhies [64], since then this model has been accepted and used extensively in the FCC literature. A different approach for deactivation functions, based on coke concentration, was proposed by Froment and Bischoff [65]. As a result; a stoichiometric relationship can be established, as demonstrated by Al-Khattaf and de Lasa [66] and Al-Khattaf et al., [63] between the amount of reactant and amount of coke produced. This allows for the use of a so-called “reactant conversion” model. This type of model has been reported to incorporate a sound mechanistic description of catalyst deactivation [67], allows for changes of chemical species without extra requirement of measuring the coke

concentration [66]. For the reactant conversion model the deactivation function is

$$\varphi = \exp(-\lambda(1 - y_B)), \quad (6)$$

where λ is catalyst deactivation constant. Substituting Eqs. (5) and (6) into Eqs. (1)–(4), we have the following first-order differential equations which are in terms of weight fractions of the species:

$$\frac{dy_B}{dt} = -\eta F_1 k_{m1} y_B y_E \frac{W_c}{V} \exp(-\lambda(1 - y_B)) \quad (7)$$

$$\frac{dy_{EB}}{dt} = [\eta F_2 k_{m1} y_B y_E - \eta F_1 k_{m3} y_{EB} y_E] \frac{W_c}{V} \exp(-\lambda(1 - y_B)) \quad (8)$$

$$\frac{dy_{DEB}}{dt} = [\eta F_3 k_{m3} y_{EB} y_E - \eta F_1 k_{m5} y_{DEB} y_E] \frac{W_c}{V} \exp(-\lambda(1 - y_B)) \quad (9)$$

$$\frac{dy_{TEB}}{dt} = \eta F_4 k_{m5} y_{DEB} y_E \frac{W_c}{V} \exp(-\lambda(1 - y_B)) \quad (10)$$

F_1 , F_2 , F_3 and F_4 are lumped constants given below:

$$F_1 = \frac{W_{hc}}{VMW_E}$$

$$F_2 = \frac{MW_{EB} W_{hc}}{VMW_B MW_E}$$

$$F_3 = \frac{MW_{DEB} W_{hc}}{VMW_{EB} MW_E}$$

$$F_4 = \frac{MW_{TEB} W_{hc}}{VMW_{DEB} MW_E}.$$

Eqs. (7)–(10) contain seven parameters, k_{m1} , k_{m2} , k_{m3} , E_{m1} , E_{m2} , E_{m3} and λ , which are to be determined by fitting into experimental data.

The temperature dependence of the rate constants was represented with the centered temperature form of the Arrhenius equation, i.e.

$$k_i = k_{oi} \exp \left[\frac{-E_i}{R} \left(\frac{1}{T} - \frac{1}{T_o} \right) \right]. \quad (11)$$

Since the experimental runs were done at 250, 275 and 300 °C, T_o was calculated to be 275 °C, where T_o is an average temperature introduced to reduce parameter interaction [68], k_{oi} is the rate constant for reaction i at T_o , W_c is the weight of catalyst and E_i is the activation energy for reaction i .

4.2. Model development for ethylation reaction over ZSM-5-based catalyst (Z-catalyst)

A kinetic model development for benzene ethylation over ZSM-5-based catalyst using an activity decay model based on reactant conversion, which is based on Scheme 3, was developed for the ethylation reaction over ZSM-5. The slight increase in toluene formation noticed at elevated temperature, which is probably due

to cracking of ethylbenzene, was not accounted for in the kinetic model development.

Therefore, k_{x2} , k_{x4} and $k_{x5} \approx 0$, (where $x = z$ in the case of ZSM-5-based catalyst). The following set of species balances and catalytic reactions can be written as follows:

Rate of disappearance of benzene:

$$-\frac{V}{W_c} \frac{dC_B}{dt} = \eta k_{z1} C_B C_E \varphi \quad (12)$$

Rate of formation of ethylbenzene:

$$\frac{V}{W_c} \frac{dC_{EB}}{dt} = (\eta k_{z1} C_B C_E - \eta k_{z3} C_{EB} C_E) \varphi \quad (13)$$

Rate of formation of diethyl benzene:

$$\frac{V}{W_c} \frac{dC_{DEB}}{dt} = \eta k_{z3} C_{EB} C_E \varphi. \quad (14)$$

Substituting Eqs. (5) and (6) into Eqs. (12)–(14) results in the following first-order differential equations which are in terms of weight fractions of the species:

$$\frac{dy_B}{dt} = -\eta H_1 k_{z1} y_B y_E \frac{W_c}{V} \exp(-\lambda(1 - y_B)) \quad (15)$$

$$\frac{dy_{EB}}{dt} = [\eta H_2 k_{z1} y_B y_E - \eta H_1 k_{z3} y_{EB} y_E] \frac{W_c}{V} \exp(-\lambda(1 - y_B)) \quad (16)$$

$$\frac{dy_{DEB}}{dt} = \eta H_3 k_{z3} y_{EB} y_E \frac{W_c}{V} \exp(-\lambda(1 - y_B)) \quad (17)$$

H_1 , H_2 and H_3 are lumped constants given below:

$$H_1 = \frac{W_{hc}}{VMW_E}$$

$$H_2 = \frac{MW_{EB} W_{hc}}{VMW_B MW_E}$$

$$H_3 = \frac{MW_{DEB} W_{hc}}{VMW_{EB} MW_E}.$$

Similar assumptions used in the kinetic model development for benzene ethylation over mordenite-based catalyst are also applicable in the ethylation of benzene with ethanol over ZSM-5-based catalyst. Eqs. (15)–(17) contain five parameters; k_{z1} , k_{z2} , E_{z1} , E_{z2} and λ , which are to be determined by fitting into experimental data.

4.3. Model development for ethylation reaction over SSZ-33-based catalyst

In accordance with the products obtained in the ethylation reaction of benzene with ethanol over SSZ-33 (Table 4), a suitable kinetic model based on Scheme 3 was developed. Diethylbenzene was not accounted for in the model development due to the inconsistent and insignificant amount of DEB noticed in the ethylation reaction over SSZ-33, except at 250 °C, during which traces of DEB were observed.

Therefore, k_{x3} , k_{x4} and $k_{x5} \approx 0$ (due to absence of TEB), where $x = s$ in the case of SSZ-33-based catalyst. The following set of species balances and catalytic reactions can be written as follows:

Rate of disappearance of benzene:

$$-\frac{V}{W_c} \frac{dC_B}{dt} = \eta k_{s1} C_B C_E \varphi \quad (18)$$

Rate of formation of ethylbenzene:

$$\frac{V}{W_c} \frac{dC_{EB}}{dt} = (\eta k_{s1} C_B C_E - \eta k_{s2} C_{EB}) \varphi \quad (19)$$

Rate of formation of toluene:

$$\frac{V}{W_c} \frac{dC_T}{dt} = \eta k_{s2} C_{EB} \varphi \quad (20)$$

Substituting Eqs. (5) and (6) into Eqs. (18)–(20) results in the following first-order differential equations which are in terms of weight fractions of the species:

$$\frac{dy_B}{dt} = -\eta G_1 k_{s1} y_B y_E \frac{W_c}{V} \exp(-\lambda(1 - y_B)) \quad (21)$$

$$\frac{dy_{EB}}{dt} = [\eta G_2 k_{s1} y_B y_E - \eta k_{s2} y_{EB}] \frac{W_c}{V} \exp(-\lambda(1 - y_B)) \quad (22)$$

$$\frac{dy_T}{dt} = \eta G_3 k_{s2} y_{EB} \frac{W_c}{V} \exp(-\lambda(1 - y_B)). \quad (23)$$

G_1 , G_2 and G_3 are lumped constants given below.

$$G_1 = \frac{W_{hc}}{VMW_E}$$

$$G_2 = \frac{MW_{EB} W_{hc}}{VMW_B MW_E}$$

$$G_3 = \frac{MW_T}{MW_{EB}}.$$

The above proposed model equations were based on the simplified assumptions stated for both mordenite and ZSM-5-based catalysts, discussed earlier in Section 4.1. Contained in Eqs. (21)–(23) are five parameters to be determined by fitting into experimental data.

4.4. Model development for ethylation reaction over TNU-9-based catalyst

Based on the product distribution presented in Table 5, in which both ethylation and cracking reaction occur in the ethylation of benzene with ethanol over TNU-9-based catalyst, a kinetic model based on Scheme 3 was developed. Therefore, $k_{x5} \approx 0$ (due to absence of TEB), where $x = TNU$ in the case of TNU-9-based catalyst. The following set of species balances and catalytic reactions can be written as follows:

Rate of disappearance of benzene:

$$-\frac{V}{W_c} \frac{dC_B}{dt} = \eta k_{TNU-1} C_B C_E \varphi \quad (24)$$

Rate of formation of ethylbenzene:

$$\frac{V}{W_c} \frac{dC_{EB}}{dt} = (\eta k_{TNU-1} C_B C_E - (\eta k_{TNU-2} C_{EB} + \eta k_{TNU-3} C_{EB} C_E)) \varphi \quad (25)$$

Rate of formation of toluene:

$$\frac{V}{W_c} \frac{dC_T}{dt} = \eta k_{TNU-2} C_{EB} \varphi \quad (26)$$

Rate of diethylbenzene formation:

$$\frac{V}{W_c} \frac{dC_{DEB}}{dt} = (\eta k_{TNU-3} C_{EB} C_E - \eta k_{TNU-4} C_{DEB}) \varphi. \quad (27)$$

Substituting Eqs. (5) and (6) into Eqs. (24)–(27) gives the following first-order differential equations which are in terms of weight fractions of the species:

$$\frac{dy_B}{dt} = -\eta S_1 k_{TNU-1} y_B y_E \frac{W_c}{V} \exp(-\lambda(1 - y_B)) \quad (28)$$

$$\frac{dy_{EB}}{dt} = [\eta S_2 k_{TNU-1} y_B y_E - (\eta k_{TNU-2} y_{EB} + \eta S_1 k_{TNU-3} y_{EB} y_E)] \times \frac{W_c}{V} \exp(-\lambda(1 - y_B)) \quad (29)$$

Table 6
Estimated kinetic parameters for mordenite catalyst based on reactant conversion (RC model).

| Parameters | Values | | | |
|--|----------|----------|----------|-----------|
| | k_{m1} | k_{m2} | k_{m3} | λ |
| E_i (kJ/mol) | 59.87 | 16.08 | 16.63 | 3.03 |
| 95% CL | 3.61 | 6.54 | 9.61 | 1.12 |
| $k_{0i}^a \times 10^3$ [(m ³ /kg of catalyst .s)] | 0.0065 | 0.0574 | 0.0712 | |
| 95% CL $\times 10^3$ | 0.0030 | 0.0259 | 0.0345 | |

^a Pre-exponential factor as obtained from Eq. (11); unit for second order (m⁶/kg of catalyst.s).

$$\frac{dy_T}{dt} = \eta S_3 k_{TNU-2} y_{EB} \frac{W_c}{V} \exp(-\lambda(1 - y_B)) \quad (30)$$

$$\frac{dy_{DEB}}{dt} = (\eta S_4 k_{TNU-3} y_{EB} y_E - \eta k_{TNU-4} y_{DEB}) \frac{W_c}{V} \exp(-\lambda(1 - y_B)). \quad (31)$$

S_1, S_2, S_3 and S_4 are lumped constants given below:

$$S_1 = \frac{W_{hc}}{VMW_E}$$

$$S_2 = \frac{MW_{EB} W_{hc}}{VMW_B MW_E}$$

$$S_3 = \frac{MW_T}{MW_{EB}}$$

$$S_4 = \frac{MW_{DEB} W_{hc}}{VMW_{EB} MW_E}$$

Similar assumptions used in the kinetic model development for benzene ethylation over mordenite-, SSZ-33- and ZSM-5-based catalyst are also applicable to the model development for ethylation of benzene with ethanol over TNU-9-based catalyst. Eqs. (28)–(31) contain nine parameters; k_{TNU-1} – k_{TNU-4} , E_{TNU-1} – E_{TNU-4} and λ , which are to be determined by fitting into experimental data.

4.5. Discussion of kinetic modeling results

The kinetic parameters k_{0i} , E_i , and λ for the ethylation reaction were obtained using nonlinear regression (MATLAB package). The values of the model parameters along with their corresponding 95% confidence limits (CLs) are shown in Tables 6, 8, 10 and 11 (RC model), while the resulting cross-correlation matrices are also given in Table 7 for mordenite-based catalyst and Table 9 for ZSM-5-based catalyst.

Based on the correlation matrices of the regression analysis presented in Table 7 for ethylation of benzene over mordenite, it shows the very low correlations between k_{m1} – k_{m3} and E_{m1} – E_{m3} and E_{m1} – E_{m3} and λ and the moderate correlation between k_{m1} – k_{m3} and λ . Similarly, Table 9 reports the very low correlations between k_{z1} , k_{z2} and E_{z1} , E_{z2} and E_{z1} , E_{z2} , and λ . It can be observed that in the cross-correlation matrices presented in this study, most of the coefficients remain in the low level with only a few exceptions.

Comparing the energies of activation for benzene ethylation over mordenite (59.87 kJ/mol), ZSM-5 (17.12 kJ/mol), SSZ-33 (12.29 kJ/mol) and TNU-9-based catalyst (10.44 kJ/mol), it can be

Table 7
Correlation matrix for benzene ethylation over mordenite-based catalyst.

| | k_{m1} | E_{m1} | λ | k_{m2} | E_{m2} | λ | k_{m3} | E_{m3} | λ |
|--------------|----------|----------|-----------|----------|----------|-----------|----------|----------|-----------|
| $k_{m1,2,3}$ | 1.0000 | 0.5846 | 0.8903 | 1.0000 | 0.3145 | 0.7968 | 1.0000 | −0.1222 | 0.6900 |
| $E_{m1,2,3}$ | 0.5846 | 1.0000 | −0.5951 | 0.3145 | 1.0000 | −0.3560 | −0.1222 | 1.0000 | 0.1822 |
| λ | 0.8903 | −0.5951 | 1.0000 | 0.7968 | −0.3560 | 1.0000 | 0.6900 | 0.1822 | 1.0000 |

Table 8
Estimated kinetic parameters for ZSM-5 catalyst based on reactant conversion (RC model).

| Parameters | Values | | |
|---|----------|----------|-----------|
| | k_{z1} | k_{z2} | λ |
| E_i (kJ/mol) | 17.12 | 8.90 | 2.28 |
| 95% CL | 2.64 | 5.80 | 0.98 |
| $k_{0i}^a \times 10^3$ [m ³ /(kg of catalyst.s)] | 0.0132 | 0.0310 | |
| 95% CL $\times 10^3$ | 0.0069 | 0.0164 | |

^a Pre-exponential factor as obtained from Eq. (11); unit for second order (m⁶/kg of catalyst.s).

Table 9
Correlation matrix for benzene ethylation over ZSM-5-based catalyst.

| | k_{z1} | E_{z1} | λ | k_{z2} | E_{z2} | λ |
|------------|----------|----------|-----------|----------|----------|-----------|
| $k_{z1,2}$ | 1.0000 | 0.2295 | 0.7937 | 1.0000 | −0.1668 | 0.8922 |
| $E_{z1,2}$ | 0.2295 | 1.0000 | 0.2332 | −0.1668 | 1.0000 | 0.4619 |
| λ | 0.7937 | 0.2332 | 1.0000 | 0.8922 | 0.4619 | 1.0000 |

Table 10
Estimated kinetic parameters for SSZ-33 catalyst based on reactant conversion (RC model).

| Parameters | Values | | |
|---|----------|----------|-----------|
| | k_{s1} | k_{s2} | λ |
| E_i (kJ/mol) | 12.29 | 67.97 | 2.94 |
| 95% CL | 4.72 | 10.57 | 0.75 |
| $k_{0i}^a \times 10^3$ [m ³ /(kg of catalyst.s)] | 0.0569 | 3.0000 | |
| 95% CL $\times 10^3$ | 0.0193 | 0.6512 | |

^a Pre-exponential factor as obtained from Eq. (11); unit for second order (m⁶/kg of catalyst.s).

inferred that the high energy of activation noticed over mordenite-based catalyst as compared with all other catalysts used in this study is anticipated, since in mordenite-based catalyst, the cross channels are sufficiently small and with respect to hydrocarbons, the structure is effectively one-dimensional and may be regarded as an array of parallel, noninterconnecting channels [58].

Comparing this to the three-dimensional pore structure of ZSM-5 [69], containing interconnected channels of 10-ring parallel to [1 0 0] (5.1 Å × 5.5 Å) and to [0 1 0] (5.3 Å × 5.6 Å), which permits complete access from one pore to all others in the structure, thereby permitting the entering of feed molecules as well as moving out of the product molecules, a much lower apparent energy of activation is expected over ZSM-5 as compared with mordenite-based catalyst.

Considering SSZ-33-based catalyst [52], which contains 12- and 10-ring interconnected channels of 6.4 Å × 7.0 Å, 5.9 Å × 7.0 Å (12-ring parallel to [0 0 1] and [1 0 0], respectively, and 4.5 Å × 5.1 Å (10 MR parallel to [0 1 0]), a lower apparent activation energy for benzene ethylation is expected, as compared with the medium pore (10-ring) ZSM-5 zeolite. It can be observed that over mordenite and ZSM-5-based catalysts, benzene ethylation was found to be higher than the apparent activation energy needed to form DEB, as a result of ethylbenzene ethylation. The difference in apparent activation energy for benzene ethylation (59.87 and 17.12 kJ/mol) and ethylbenzene ethylation (16.08 and 8.90 kJ/mol) noticed over both

Table 11
Estimated kinetic parameters for TNU-9 catalyst based on reactant conversion (RC model).

| Parameters | Values | | | | |
|--|--------------------|--------------------|--------------------|--------------------|-----------|
| | $k_{\text{TNU-1}}$ | $k_{\text{TNU-2}}$ | $k_{\text{TNU-3}}$ | $k_{\text{TNU-4}}$ | λ |
| E_i (kJ/mol) | 10.44 | 15.20 | 24.51 | 12.82 | 2.44 |
| 95% CL | 2.71 | 1.36 | 5.79 | 3.52 | 0.93 |
| $k_0 \times 10^4$ [m ³ /(kg of catalyst.s)] | 0.116 | 2.700 | 0.362 | 16.67 | |
| 95% CL $\times 10^4$ | 0.067 | 0.060 | 0.022 | 8.13 | |

^a Pre-exponential factor as obtained from Eq. (11); unit for second order (m⁶/kg of catalyst s).

catalysts is not unusual, since alkylation reactions of long substituted benzene generally occur with greater ease compared to their shorter substituted counterparts [47].

It is evident from Tables 4 and 5 that the increase in temperature leads to a larger fraction of cracking products, which clearly validate the higher apparent activation energies noticed for EB cracking (67.97 and 15.20 kJ/mol) over SSZ-33 and TNU-9-based catalysts, respectively, as compared with the apparent energies of activation obtained for benzene ethylation (12.29 and 10.44 kJ/mol) over both catalysts. This important difference in energies of activation is in perfect agreement with previous study [38]. Sridevi et al. [61] and Barman et al. [18] reported an apparent energy of activation of 60.03 and 56 kJ/mol for ethylation of benzene over AlCl₃ impregnated 13× zeolite and cerium exchange NaX zeolite, respectively. These values are in agreement, or have the same order with the value obtained in this present study for benzene ethylation over mordenite-based catalyst.

Graphical comparisons between experimental and model predictions for the reactant conversion model (RC) based on the optimized parameters for mordenite and ZSM-5 are shown in Figs. 3 and 4, respectively. It can be seen that the model predictions compared very well with the experimental data.

5. Conclusions

The following conclusions can be drawn from the ethylation reaction of benzene with ethanol over ZSM-5-, TNU-9-, SSZ-33- and mordenite-based catalyst.

1. The zeolite structure in combination with the reaction temperature determines the types of reactions that occur.
2. Ethylbenzene selectivity was found to be highest in the ethylation reaction over ZSM-5-based catalyst as compared to its ethylation over all other zeolite catalysts.
3. SSZ-33-based catalyst produced the highest benzene conversion as compared to its conversion over ZSM-5-, TNU-9- and mordenite-based catalyst.
4. Considerable amount of toluene was obtained in the ethylation over SSZ-33-based catalyst, while negligible amount was noticed over mordenite-based catalyst. It can be concluded that acidity plays a major role in toluene formation over these zeolites.
5. An increase in the concentration of Lewis acid sites was observed after modification of the parent zeolites with alumina binder.
6. In the ethylation reaction over mordenite- and ZSM-5-based catalyst, the apparent activation energy for EB ethylation (E_{m2} and E_{z2}) was found to be lower than the apparent energy of activation obtained for benzene ethylation (E_{m1} and E_{z1}), which shows that reactivity of the alkylbenzenes increases as the number of ethyl group per benzene ring increases.
7. Kinetic parameters for benzene ethylation over all the studied zeolites were calculated using the catalyst activity decay function based on reactant conversion. The apparent activation

energies for benzene ethylation were found to decrease as follows: $E_{m1} > E_{z1} > E_{s1} > E_{\text{TNU-1}}$.

Acknowledgements

The authors acknowledge the financial support provided by King AbdulAziz City for Science and Technology for this research under the Refining & Petrochemicals Program of the National Science and Technology Plan (NSTP) for the year 2009 (09-PETE86-4). We are grateful for the support from Ministry of Higher Education, Saudi Arabia for the establishment of the Center of Research Excellence in Petroleum Refining and Petrochemicals at King Fahd University of Petroleum and Minerals (KFUPM). The authors thank J. Cejka and M. Kubu (Heyrovsky Institute of Physical Chemistry, Prague, Czech Republic) for providing zeolites TNU-9 and SSZ-33 and their characterization.

References

- [1] J. Cejka, B. Wichterlova, Catal. Rev. 44 (2002) 375–421.
- [2] T. Degnan, Appl. Catal. A 221 (2001) 283–294.
- [3] N.M. Tukur, S. Al-Khattaf, Catal. Lett. 131 (2009) 225–233.
- [4] J. Weikamp, L. Puppe, Catalysis and Zeolites, Springer, Berlin, 1999, pp. 81.
- [5] C. Perego, P. Ingallina, Catal. Today 73 (2002) 3–22.
- [6] N.Y. Chen, W.E. Garwood, Catal. Rev. Sci. Eng. 28 (1986) 185–264.
- [7] A. Corma, M.E. Domine, S. Valencia, J. Catal. 215 (2003) 294–304.
- [8] N. Zilkova, M. Bejblova, B. Gil, S.I. Zones, A.W. Burton, C.Y. Chen, Z. Musilova-Pavlackova, G. Kosova, J. Cejka, J. Catal. 266 (2009) 79–91.
- [9] S. Kato, K. Nakagawa, N. Ikenaga, T. Suzuki, Catal. Lett. 73 (2001) 2–4.
- [10] P.B. Venuto, L.A. Hamilton, P.S. Landis, J.J. Wise, J. Catal. 5 (1966) 81–98.
- [11] C.G. Wight, US Patent 4, 169 (1979) 111.
- [12] G. Bellusi, G. Pazzuconi, C. Perego, G. Girotti, G. Terzoni, J. Catal. 157 (1995) 227–234.
- [13] L. Forni, G. Cremona, F. Missineo, G. Bellusi, C. Perego, G. Pazzuconi, Appl. Catal. 121 (1995) 261–272.
- [14] J. Cejka, B. Wichterlova, S. Bednarova, Appl. Catal. 79 (1991) 215–226.
- [15] M. Raimondo, G. Perez, A. De Stefanis, A.A.G. Tomilinson, O. Ursini, Appl. Catal. A 164 (1997) 119–126.
- [16] V.R. Vijayaraghavan, K.J.A. Raj, J. Mol. Catal. A 207 (2004) 41–50.
- [17] N.N. Binitha, S. Sugunan, Micropor. Mesopor. Mater. 93 (2006) 82–89.
- [18] S. Barman, N.C. Pradhan, J.K. Basu, Indian Chem. Eng. A 48 (2006) 10–17.
- [19] R.T. Sebulsky, A.M. Henke, Ind. Eng. Chem. Process Des. Dev. 10 (1971) 272–279.
- [20] T.J.L. Berna, D.A. Moreno, European Patent Appl. EP 0 353 (1991) 813.
- [21] L.B. Young, US Patent 4, 301 (1981) 317.
- [22] J. Cejka, A. Vondrova, B. Wichterlova, G. Vorbeck, R. Fricke, Zeolites 14 (1994) 147–153.
- [23] J. Cejka, N. Zilkova, B. Wichterlova, Collect. Czech. Chem. Comm. 61 (1996) 1115–1130.
- [24] B. Wichterlova, J. Cejka, N. Zilkova, Microporous Mat. 6 (1996) 405–414.
- [25] P.K. Bajpai, Zeolites 6 (1986) 2–8.
- [26] I.E. Maxwell, W.H.J. Stork, in: H. von Bekkum, E.M. Flanigen, J.C. Jansen (Eds.), Introduction to Zeolite Science and Practice, Elsevier, Amsterdam, 1991, p. 71.
- [27] L.D. Fernandes, J.L.F. Moneteiro, E.F. Sousa-Aguiar, A. Martinez, A. Corma, J. Catal. 177 (1998) 363–377.
- [28] J.E. Gilbert, A. Mosset, Mater. Res. Bull. 33 (1998) 997–1003.
- [29] Pierre Levesque, Le H. Dao, Appl. Catal., 53 (1989) 157–167.
- [30] J. Gao, L. Zhang, J.X. Hu, W. Li, J.G. Wang, Catal. Comm. 10 (2009) 1615–1619.
- [31] K.H. Chandawar, S.B. Kulkarni, P. Ratnaswamy, Appl. Catal. A 4 (1982) 287–295.
- [32] T. Odedairo, S. Al-Khattaf, Chem. Eng. J. 157 (2010) 204–215.
- [33] J.R. Anderson, K. Foger, T. Mole, R.A. Rajyadhyaksha, J.V. Sanders, J. Catal. 58 (1979) 114–130.
- [34] J.R. Anderson, T. Mole, V. Christov, J. Catal. 61 (1980) 477–484.
- [35] Y.S. Bhat, A.B. Halgeri, T.S.R. Prasada Rao, Ind. Eng. Chem. Res. 28 (1998) 894–899.
- [36] B. Lee, I. Wang, Ind. Eng. Chem. Prod. Res. Dev. 24 (1985) 201–208.
- [37] I. Wang, S.J. Li, J.Y. Liu, In: Int. Symp. Zeolites and Microporous Crystals, Sendai, Japan, 2 LC 01, 6–9 August 2000.
- [38] T. Odedairo, S. Al-Khattaf, Ind. Eng. Chem. Res. 49 (2010) 1642–1651.
- [39] P. Wagner, Y. Nakagawa, G.S. Lee, M.E. Davis, S. Elomari, R.C. Medurd, S.I. Zones, J. Am. Chem. Soc. (2000) 122–263.
- [40] A. Corma, F.J. Llopis, C. Martinez, G. Sastre, S. Valencia, J. Catal. 268 (2009) 9–17.
- [41] J. Cejka, N. Zilkova, S.I. Zones, M. Bejblova, 18th Saudi Japan Symposium, November, 2008.
- [42] F. Gramm, C. Baerlocher, L.B. McCusker, S.J. Warrender, P.A. Wright, B. Han, S.B. Hong, Z. Liu, T. Ohsuna, O. Terasaki, Nature 444 (2006) 79–81.
- [43] C.A. Emeis, J. Catal. 141 (1993) 347–354.
- [44] B. Gil, S.I. Zones, S.J. Hwang, M. Bejblova, J. Cejka, J. Phys. Chem. 112 (2008) 2997–3007.
- [45] de Lasa, H.I., US Patent 5, 102 (1991) 628.

- [46] D.W. Kraemer, Ph.D. Dissertation, University of Western Ontario, London, Canada, 1991.
- [47] W.W. Kaeding, *J. Catal.* 95 (1985) 512–519.
- [48] A.B. Halgeri, *Bull. Catal. Soc. India* 2 (2003) 184–193.
- [49] B. Wichterlova, J. Cejka, *Catal. Lett.* 16 (1992) 421–429.
- [50] W.W. Kaeding, G.C. Barlie, M.M. Wu, *Catal. Rev.—Sci. Eng.* 26 (1984) 597–612.
- [51] T. Tsai, S. Liu, I. Wang, *Appl. Catal. A* 181 (1999) 355–398.
- [52] F.J. Llopis, G. Sastre, A. Corma, *J. Catal.* 227 (2004) 227–241.
- [53] S. Al-Khattaf, M.A. Ali, A. Al-Amer, *Energy Fuels* 22 (2008) 243–249.
- [54] S. Rabiou, S. Al-Khattaf, *Ind. Eng. Chem. Res.* 47 (2008) 39–47.
- [55] S.B. Hong, *Catal. Surv. Asia* 12 (2008) 131–144.
- [56] S.H. Lee, D.K. Lee, C.H. Shin, Y.K. Park, P.A. Wright, W.M. Lee, S.B. Hong, *J. Catal.* 215 (2003) 151–170.
- [57] S. Al-Khattaf, Z. Musilova-Pavlackova, M.A. Ali, J. Cejka, *Top. Catal.* 52 (2009) 140–147.
- [58] C.N. Satterfield, *Heterogeneous Catalysis in Industrial Practice*, 2nd ed, Krieger Publishing Company, Malabar, Florida, 1996.
- [59] N.Y. Chen, F. Thomas Degnan, C. Morris Smith, *Molecular Transport and Reaction in Zeolites*, VCH, New York, 1994.
- [60] A.Z. Abdullah, M.Z. Abu Bakar, S. Bhatia, *The Proceedings of RSCE and 16th SOMCHE, Malaysia*, 28–30 October, 2002.
- [61] U. Sridevi, B.K. Bhaskar Rao, N.C. Pradhan, *Chem. Eng. J* 83 (2001) 185–189.
- [62] J. Wei, *J. Catal.* 76 (1982) 433–439.
- [63] S. Al-Khattaf, J.A. Atias, K. Jarosch, H. de Lasa *Chem. Eng. Sci.* 57 (2002) 4909–4920.
- [64] A. Voorhies, *Ind. Eng. Chem. Res.* 37 (1945) 318–322.
- [65] G.F. Froment, K.B. Bischoff, *Chemical Reactor Analysis and Design*, second ed., John Wiley & Sons, New York, 1979, pp. 288.
- [66] S. Al-Khattaf, H.I. de Lasa, *Ind. Eng. Chem. Res.* 40 (2001) 5398–5404.
- [67] J.A. Atias, G. Tonetto, H. de Lasa, *Ind. Eng. Chem. Res.* 42 (2003) 4162–4173.
- [68] A.K. Agarwal, M.L. Brisk, *Ind. Eng. Chem. Process Des. Dev.* 24 (1985) 203–207.
- [69] H.V. Koningsveld, H.V. Bekkum, J.C. Jansen, *Acta Crystallogr. B* 43 (1987) 127–128.